Fluid Flow Through a Solid-Liquid Dendritic Interface

M. J. STEWART AND F. WEINBERG

Fluid flow through a dendritic solid-liquid interfacial zone, during solidification, has been observed in a series of Sn-Pb alloys. It was found that liquid penetrates only a short distance into the zone, relative to the total thickness of the zone. The amount of solid present at the point of maximum penetration varies from 12 to 22 pct, and depends on the alloy concentration. Flow due to volume shrinkage, thermal convection, or solute convection well inside the zone, was not detected. Fluid flow through a wire mesh model of a thin section of the solid-liquid dendritic zone was examined. The results are not in agreement with that predicted for flow through a porous barrier, which had been found applicable to interdendritic fluid flow.

THE importance of interdendritic fluid flow during solidification has recently been pointed out by a number of investigators.[1-6] The nature and extent of this type of flow has been inferred from observations made in transparent ammonium chloride cells[2] and from particular solute segregation patterns believed to result from interdendritic flow.[4-6] No direct observations of interdendritic flow in a metal system, during solidification, have been reported. Interdendritic flow can result from a number of forces during solidification including a) volume contraction on freezing, resulting in liquid being drawn into the solid-liquid zone, b) thermal contraction of solid and liquid, c) thermal convection, d) solute convection, and e) fluid motion in the residual liquid pool due to pouring turbulence. The flow is complex, since it occurs through a network of channels whose size and configuration change with time during solidification and whose morphology is markedly dependent on the solidification parameters.

This investigation was undertaken to establish directly the extent of interdendritic fluid flow during solidification, and to relate the observed flow to that obtained through a simplified model of a solid-liquid dendritic configuration.

PROCEDURE AND OBSERVATIONS

1) Fluid Flow Through a Dendritic Solid-Liquid Interface

The general experimental procedure used in this investigation is described fully elsewhere.[7] Observations of interdendritic fluid flow during solidification were made, using radioactive tracers, by observing the depth of penetration of liquid flowing into the partially solidified dendritic region. Pb-Sn alloys were used, contained in a cell 10.8 (A) by 6.4 (B) by 0.32 (C) cm in size with AC horizontal. A temperature gradient was imposed across length A of the cell producing a natural convective flow pattern in the liquid of known configuration and velocity.[7] The ambient temperature was then lowered, maintaining the temperature difference across the cell, until solidification started at the cold side of the cell and progressed to the cell center. At this time a small amount of the same alloy, containing radioactive material, was added to the top liquid surface. After approximately 30 sec the sample was rapidly quenched, and subsequently autoradiographed to determine the distribution of the radioactive material in the cell at the time of quenching. The material investigated was pure tin and alloys of tin containing 2, 5, 12.5, and 20 wt pct Pb.

During solidification, temperatures were measured in the cell with three fine thermocouples positioned at equal intervals across A. The rate of solidification, as determined from the resultant cooling curves, was 2 to 5 cm per hr for all of the results reported here. Since an interval of only 30 sec elapsed between adding the tracer and quenching the alloy, the solid-liquid interface can be considered as effectively stationary during this time.

The typical structure of an alloy allowed to solidify under normal conditions, without quenching, is shown in Fig. 1. This is an autoradiograph of Sn-2 pct Pb containing a small amount of Tl^{204} which segregated during solidification, delineating the structure. Solidification started from the left, and a regular dendritic structure developed after approximately one-third of the metal had solidified. The primary dendrites have a spacing between 700 and 1000 μ and grow in a direction inclined to the horizontal plane. The inclination is directly related to the inclination of the solid-liquid interface as described below.

The position and shape of the solid-liquid interface in pure tin is shown in Fig. 2 where Sn^{113} was added

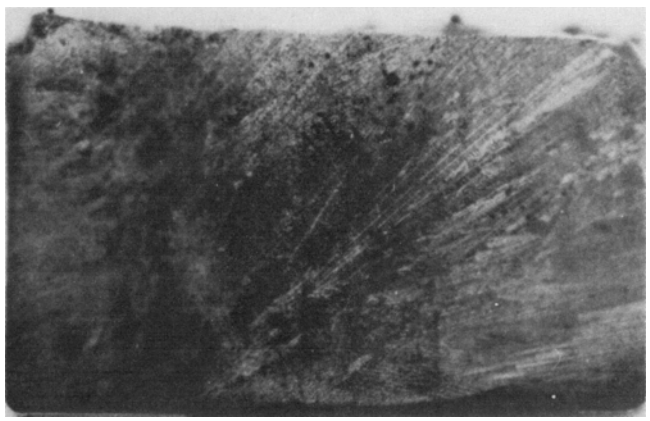

Fig. 1—Autoradiograph of Tl^{204} in Sn-2 pct Pb alloy showing the dendritic structure of the alloy.

M. J. STEWART, formerly Graduate Student, University of British Columbia, Vancouver, British Columbia, Canada, is now Research Scientist, Mines Branch, Department of Energy, Mines and Resources, Ottawa, Canada. F. WEINBERG is Professor, Department of Metallurgy, University of British Columbia.

Manuscript submitted January 14, 1971.

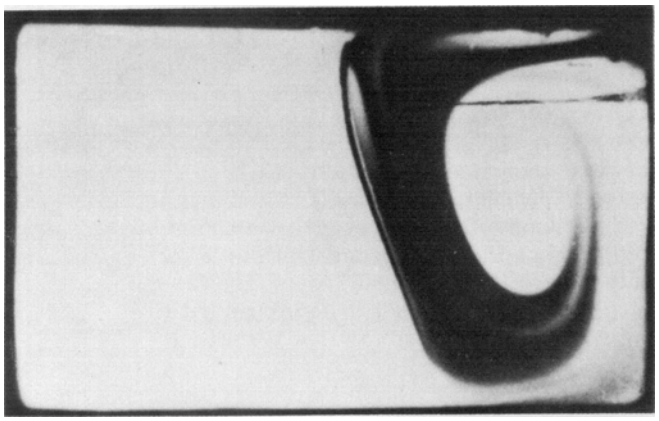

Fig. 2—Autoradiograph of Sn^{113} in tin showing smooth solid-liquid interface at left of dark region.

to the liquid when half the material had solidified and the system quenched after 30 sec. The darkened regions in the figure indicate the presence of Sn^{113} and delineate the flow pattern in the liquid. On the left side of the darkened region, the solid-liquid interface is clearly observed as smooth and sloping to the right. The interface would be vertical and linear if heat transfer across the cell was entirely due to thermal conduction. In the present case thermal convection is also present, which distorts the heat flow pattern producing isotherms which conform with the sloping interface shown in the figure.[8,9]

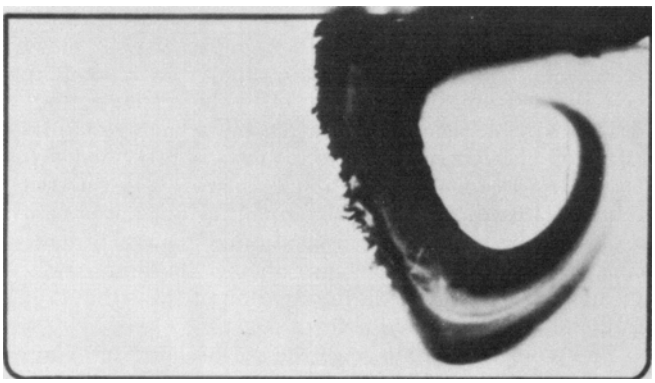

(a)

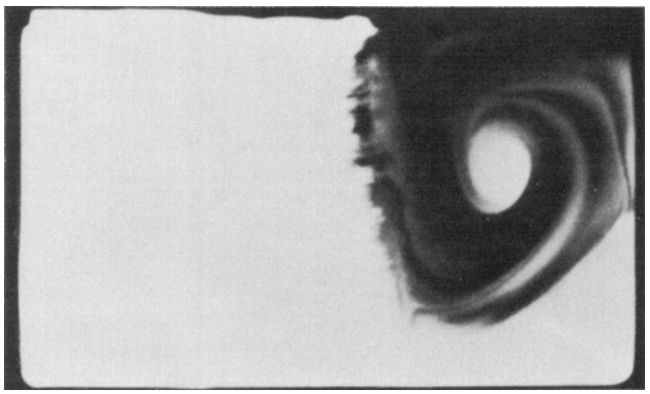

(b)

Fig. 3—Autoradiograph Tl^{204} in (*a*) Sn-2 pct Pb and (*b*) Sn-5 pct Pb showing dendritic structure of interface and flow penetration at left of dark region.

Table I. Flow Penetration into Solid-Liquid Dendritic Zone

Wt Pct Pb	Temperature Gradient in Solid-Liquid Zone, °C/cm	Distance Between *T* Liquidus and *T* Solidus, mm	Average Flow Penetration, mm
2	3.69	51	2.0
5	3.08	135	3.7
12.5	5.20	59	4.0
20	3.50	58	8.9
20	4.07	50	6.1

The solid-liquid interface in two representative alloys containing 2 and 5 wt pct Pb are shown in Figs. 3(*a*) and 3(*b*), respectively. The interface in both cases is irregular and clearly dendritic, with relatively little penetration of the liquid into the dendritic array. The amount of penetration, measured from similar autoradiographs for the alloys considered, is given in Table I along with the relevant thermal data. Comparing the observed flow penetration with the thickness of the solid-liquid region, as determined from the solidus and liquidus temperatures, it is apparent that the flow penetration is a small fraction of the thickness of the solid-liquid zone. Also the amount of penetration is relatively independent of the alloy concentration. The percent of solid present in the solid-liquid region at the deepest point of penetration of the liquid flow is shown in Fig. 4 as a function of lead content in the alloy. The values were determined from the interpolated temperature corresponding to the point of deepest penetration and the phase diagram.[10] The penetration is largest for the low concentration alloys, dropping progressively to a constant value between 12 and 20 wt pct Pb.

As a check to determine that the solid-liquid zone width obtained from the temperature measurements was correct, a fine wire was pushed into the interface, perpendicular to the plane defined by the dendrite tips immediately after the tracer was added. After quenching, the position of the tip of the wire was established by sectioning. The solid-liquid zone thickness was then determined by measuring the distance between the wire tip and the dendrite tips delineated in the corresponding autoradiograph. The results

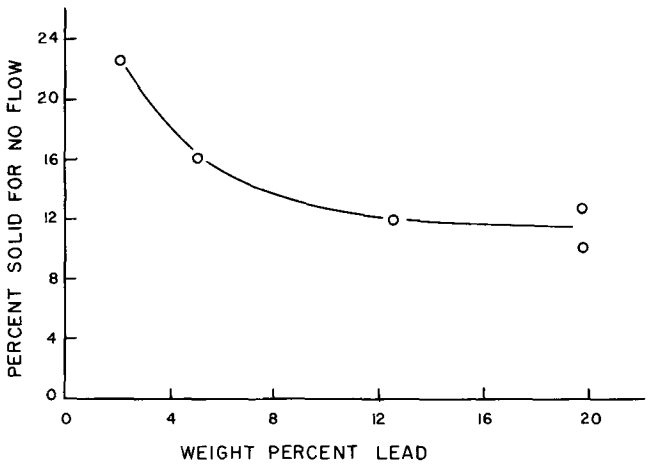

Fig. 4—Percent solid present at point of deepest liquid penetration vs lead concentration in Sn-Pb alloys.

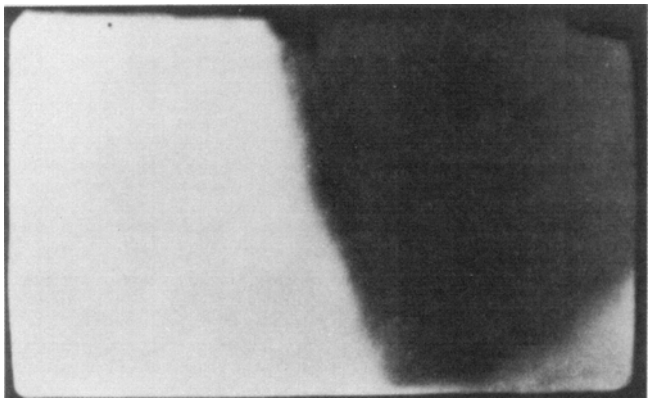

Fig. 5—Autoradiograph of Tl^{204} in Sn-2 pct Pb alloy solidified progressively without quenching.

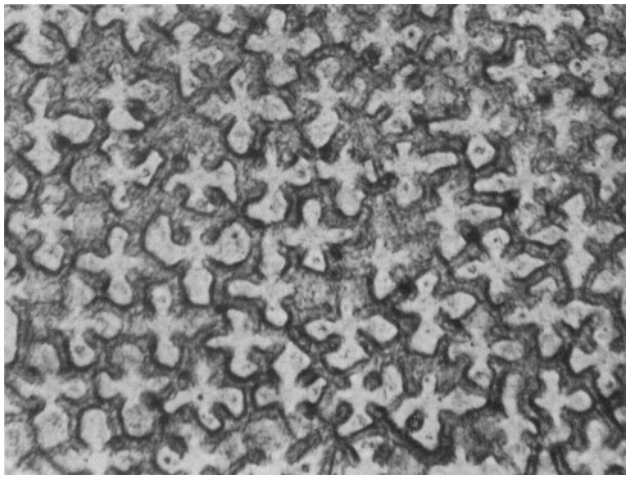

Fig. 6—Etched surface of unidirectionally cast Cu-5 pct Ni alloy sectioned on a plane perpendicular to the growth direction. Magnification 130 times.

agreed with the zone thickness determined from the thermal measurements.

Interdendritic fluid flow may occur deep in the solid-liquid zone, due, in some part, to volume shrinkage, thermal convection and solute convection. This should draw in tracer-rich liquid from the outer region of the zone, which was not observed in Fig. 3. It is possible that more time than the 30 sec allowed between introduction of the tracer and quenching is necessary to show this effect. To test this possibility, the experiment giving the autoradiograph of Fig. 3(*a*) was repeated, but without quenching the system, solidification progressing slowly to the end of the cell. Also Sn^{113} was used instead of Tl^{204} to minimize segregation on solidification. The result is shown in Fig. 5. The solid-liquid interface, as delineated by the tracer, is very similar to that shown in Fig. 3(*a*), with no apparent deeper penetration of the tracer-rich liquid. No flow pattern is observed in the tracer-rich region, as the tracer had ample time to completely mix in the liquid as solidification proceeded.

2) Fluid Flow Through a Model of a Dendritic Interface

The morphology of a solid-liquid dendritic zone during solidification is complex, since the primary

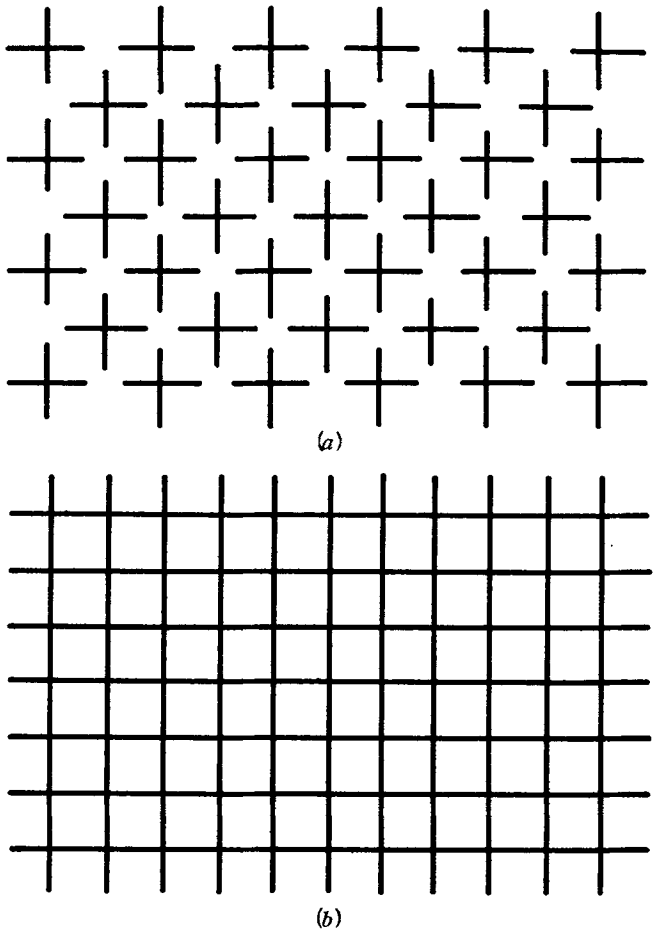

Fig. 7—(*a*) Schematic drawing of the primary dendritic network perpendicular to the growth direction shown in Fig. 6. (*b*) A continuous mesh used to approximate the dendritic network.

dendrites progressively thicken and develop secondary branches behind the leading edge of the zone. As a result, an analysis of fluid flow through such a zone is not possible at the present time. As a first approx-

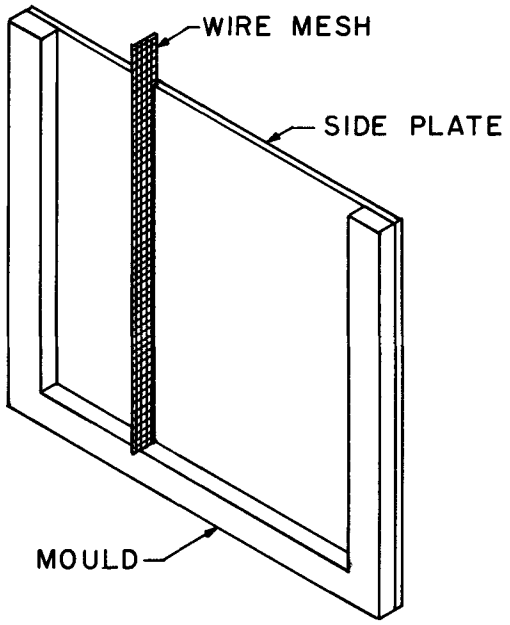

Fig. 8—Wire mesh model for observing interdendritic flow.

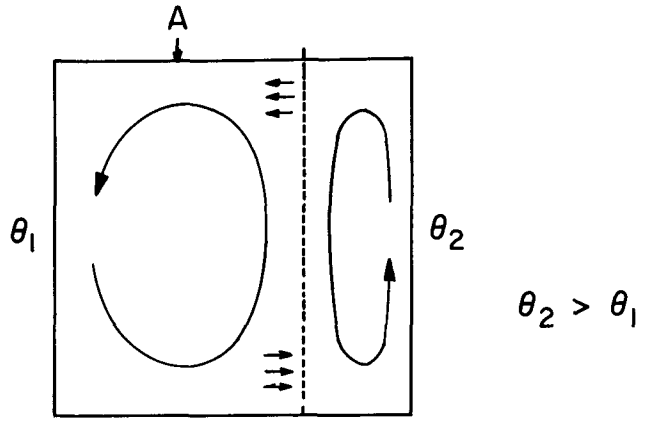

Fig. 9—The flow lines in the system of Fig. 8 showing the two flow cells and the intermesh flow, resulting from the temperature difference $\theta_2-\theta_1$.

imation, the flow through a thin section in the zone, parallel to the leading edge of the zone, is considered. The morphology of the dendritic structure in such a section for a Cu-5 pct Ni alloy cast unidirectionally and sectioned perpendicular to the primary dendrite direction is shown in Fig. 6. The dendrites in the photomicrograph are very regular and form an interlocking array. A schematic drawing of the array, with each dendrite represented by a cross, is shown in Fig. 7(*a*), which can reasonably be represented, to a first approximation, by the square grid shown in Fig. 7(*b*). Fluid flow through a square grid array can be examined experimentally, by inserting a square wire mesh into the path of liquid flowing under a known driving force and determining the amount of liquid which penetrates the mesh.

Experiments of this type were carried out in the present investigation by inserting a wire mesh into the liquid cell, as shown in Fig. 8 (Note that one side plate is not included to show the mesh-mold configuration). When a temperature difference is imposed across the mold, a flow pattern develops, as shown in Fig. 9. Flow will occur through the wire mesh from left to

Table II. Data on Wire Meshes Used in Flow Experiments and Fraction Flowed Results

	Mesh Properties				Experimental Results		
Sample Number	Mesh Number, Wires/in.	Wire Diameter, d_w, mm	Wire Spacing, S_a, mm	Hole Size, h_a, mm	Counts, Large Cell	Counts, Small Cell	Fraction Flowed, f
1	100	0.114	0.254	0.140	9559	1692	0.107
2	100	0.102	0.254	0.152	7368	662	0.082
3	80	0.165	0.317	0.152	11374	266	0.023
4	80	0.127	0.317	0.191	8445	409	0.046
5	60	0.241	0.424	0.183	7384	259	0.034
6	60	0.178	0.424	0.246	7348	720	0.089
7	40	0.279	0.635	0.356	6934	311	0.043
8	40	0.216	0.635	0.419	10330	1149	0.100
9	30	0.330	0.846	0.516	6569	279	0.041
10	30	0.254	0.846	0.592	7121	2410	0 253

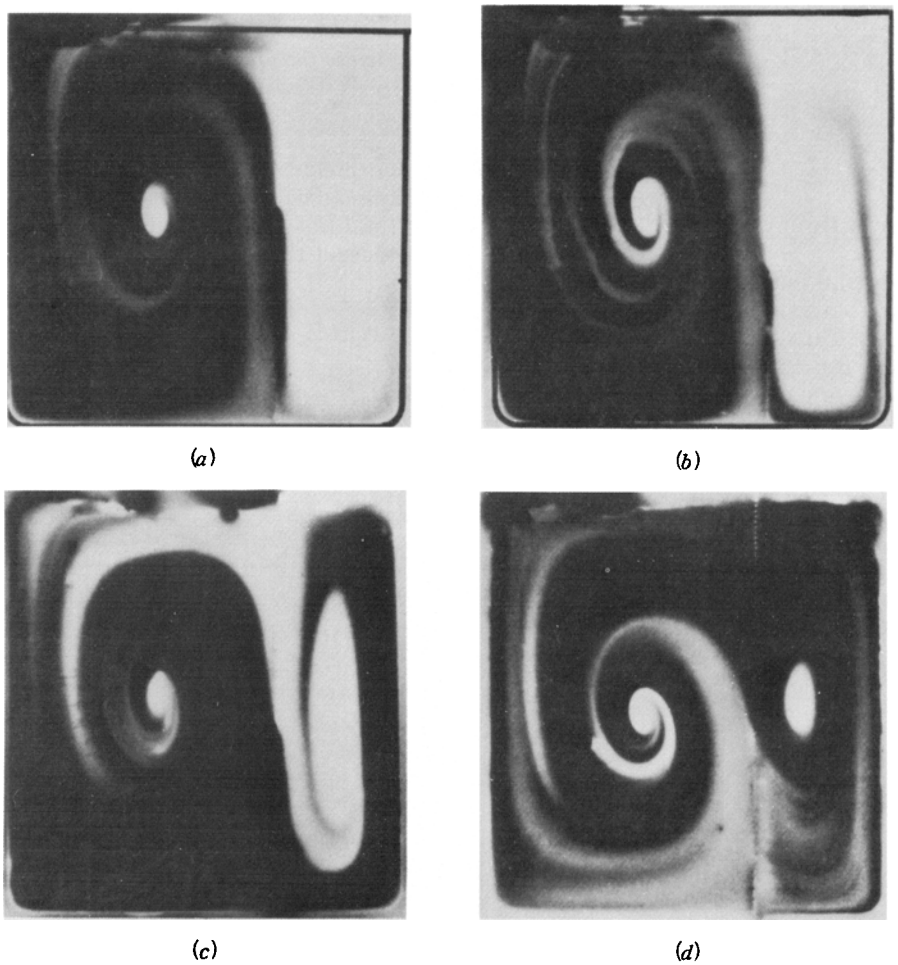

Fig. 10—Autoradiograph of Tl^{204} in lead, 120 sec after the tracer was introduced into the left cell, for the wire mesh sample listed in Table II. Sample No. (*a*) 5; (*b*) 4; (*c*) 2; and (*d*) 10.

right near the bottom of the cell and in the opposite direction near the top, as indicated by the arrows in the figure. The wire meshes used were square woven and were either of copper or phosphor bronze. Their dimensions are listed in Table II. Prior to use, the meshes were coated with a soldering flux and dipped into a lead bath to provide a good wetting surface in the experiment. The liquid used in the mold was pure lead and the flow was observed by adding radioactive Tl^{204}. A constant temperature difference of 6.05 ± 0.05°C was imposed across the mold providing a constant driving force. It was established that the wire mesh was not significantly dissolved in the molten lead, and that flow did not occur around the mesh.

The flow patterns for a series of wire meshes is shown in Fig. 10. Almost no flow occurs through sample 5 (60 mesh), increasing flow through samples 4 and 2 (80 and 100 mesh), and almost complete flow through sample 10 (30 mesh).

A more quantitative value of the amount of flow through the wire mesh was made by measuring the total activity emanating from the sample face on either side of the wire mesh using a scintillation counter. A lead shield was used to block off one side of the sample when the other side was counted. The degree of intermesh flow was taken as the ratio of the number of counts from the small cell, over the combined counts from the small and large cells. This is essentially the fraction of the tracer that has gone through the mesh. The results are listed in Table II as the fraction flowed, f.

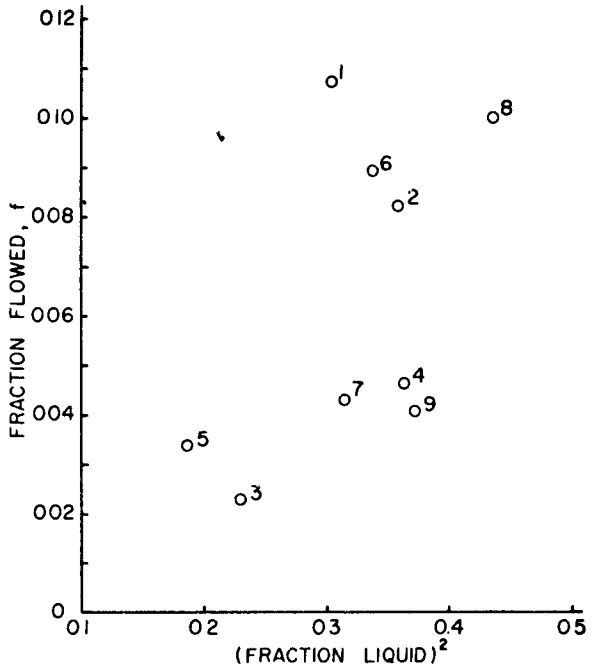

Fig. 11—Fraction of liquid which flowed through wire mesh vs square of fraction liquid in the mesh. The number at each point is the sample number listed in Table II.

According to the results of Piwonka and Flemings,[11] for a constant driving force, the flow through a solid-liquid region should be proportional to the square of the fraction liquid. In the present case the driving force, thermal convection, is constant. Fig. 11 is a plot of the fraction flowed vs the square of the fraction liquid for the wire mesh. It is seen that the plot cannot be resolved into any relationship due to the scatter of the points.

DISCUSSION AND SUMMARY

The interdendritic fluid flow in actual Pb-Sn alloys due to residual liquid pool convection has been observed. The flow penetrates to a distance corresponding to 12 to 22 pct solid in the solid-liquid zone, in castings with a primary dendrite spacing of 700 to 1000 μ. From the comparison of Figs. 3(a) and 5, if there was any flow into the solid-liquid zone due to volume changes, thermal convection, or solute convection in the inner regions of the solid-liquid zone, it does not cause any long range movement of liquid. The flow rates must therefore be extremely small.

The results of the wire mesh model indicate that a simple relationship does not satisfy the experimental results for the liquid metal flow through a porous barrier. The reasons for this are unknown. A first-order analysis has been carried out elsewhere[8] relating the wire mesh model quantitatively to the Pb-Sn alloy results in which a limited correlation was possible. The important point is that if an experimental model can be devised, which is a better representative of an actual solid-liquid dendritic zone than adopted in this investigation, then the technique presented here could prove very useful.

REFERENCES

1 R Mehrabian, M. Keane, and M. C. Flemings *Met Trans.*, 1970, vol. 1, p. 1209.
2. R. J MacDonald and J. D. Hunt: *Trans. TMS-AIME,* 1969, vol. 245, p. 1993.
3. N. Standish and G. Lang *J. Aust. Inst. Metals,* 1970, vol. 15, p. 120.
4. M. C. Flemings and G. E. Nereo: *Trans. TMS-AIME,* 1967, vol. 239, p. 1449.
5 M. C. Flemings, R. Mehrabian, and G. E. Nereo: *Trans. TMS-AIME,* 1968, vol. 242, p. 41.
6. M. C. Flemings and G. E. Nereo *Trans. TMS-AIME,* 1968, vol. 242, p. 50.
7. M. J. Stewart and F. Weinberg: *Trans. TMS-AIME,* 1969, vol. 245, p. 2108.
8. M. J. Stewart: Ph.D. Thesis, 1970, The University of British Columbia, Vancouver, Canada.
9. J. Szekely and P. S Chhabra *Met. Trans.*, 1970, vol. 1, p. 1195.
10. M. Hansen: *Constitution of Binary Alloys,* 2nd ed., McGraw-Hill Book Co., New York, 1968.
11. T. S. Piwonka and M. C. Flemings: *Trans. TMS-AIME,* 1966, vol. 236, p. 1157.